Paramagnetic-resonance studies of local fluctuations in $SrTiO_3$ above T_c

G. F. Reiter,* W. Berlinger, and K. A. Müller
IBM Zurich Research Laboratory, CH-8803 Rüschlikon, Switzerland

P. Heller
Physics Department, Brandeis University, Waltham, Massachusetts 02154
(Received 20 June 1979)

Detailed studies on electron paramagnetic resonance (EPR) of the Fe^{3+}-V_O center in a monodomain single crystal of $SrTiO_3$, have been made for $T_c < T < 295$ K. By adjusting the direction of the applied magnetic field, the sensitivity of the EPR frequency to the local rotation angles of the oxygen octahedra can be varied. A comprehensive theoretical analysis of this technique was carried out, making it possible to separate the secular, nonsecular, and background effects. We then showed from the angular dependence of the observed secular linewidth, that the slow-motion regime is obtained throughout the critical region $T_c < T < T_c + 11$ K, i.e., the local fluctuations are static on the time scale of the EPR relaxation itself. The EPR line shapes in this region then provide a direct measure of the distribution of local rotation angles. An upper limit of 6 MHz is placed upon the characteristic frequency of the local-rotation fluctuations in this region. The characteristic collective-mode relaxation rate, i.e., the "central-peak" width, should be about an order of magnitude narrower.

I. INTRODUCTION

Since Riste *et al.*[1] first observed a central peak in the neutron scattering cross section of $SrTiO_3$, later studied by Shapiro *et al.*,[2] there have been numerous experiments to determine a width of the peak[3] and considerable theoretical efforts concerning its origin.[4] Central peaks have been found in the spectral function of other materials[5] and are now recognized as a dominant feature of a structural phase transition.

The width of the central peak is one of the primary issues in any theoretical interpretation and, as of this time, there is no conclusive evidence that the width is not zero. The present work began as an attempt to resolve the central-peak linewidth using the EPR of a magnetic impurity in $SrTiO_3$ as a probe. The early results of the experiments had a natural interpretation that indicated a linewidth of the order of 60 MHz at a temperature of $T_c + 4$ K ($T_c = 105.6 \pm 0.2$ K).[6] This interpretation should now be abandoned; further data and a more detailed analysis show conclusively that the local fluctuation rate is below the limits of resolution of the experiment, placing an upper limit on its width of < 6 MHz at temperatures up to $T_c + 11$ K.[7] This is far below the limits of resolution of previous experiments. The experiment has provided, as a positive result, a direct measurement of the distribution of the local value of the order parameter for a range of temperature $\Delta T/T_c \lesssim 0.10$, and can provide a test for quantitative predictions of theoretical models.

In Sec. II we describe the experiment. Section III is the theoretical analysis needed to interpret the data. Section IV is the analysis of the data, and Sec. V a discussion of possible theoretical interpretations.

II. EXPERIMENTAL

A. Equipment

The spectrometer used was of the single-sideband superheterodyne-type working at 19.5 GHz, together with a low-frequency 73-Hz Zeeman modulation. The cavity system, including the temperature controller was the same as described earlier.[8] The thermal stability achieved herewith was better than 0.01 K, whereas the absolute temperature was measured to 0.1 K.

On-line signal recording was done by analog *x-y* plotting parallel with a digital accumulation on a multichannel analyzer (MCA).[9] The interface for data read out was an IBM Research APL device coupler connected via a telephone line with the in-house IBM 158 computer. A single EPR-line spectrum was divided into 512 channels and the *x-y* parameters, magnetic field, and absorption were stored in the MCA. Owing to its large 8192 channel capacity, 16 curves could thus be stored in the MCA memory. In case of insufficient signal-to-noise ratio, a multiscan sequence could be initiated; thus the MCA acted as signal averager as well as a buffer stage enabling the spectra to be recorded at a high rate of 512 points per half a minute scan time. The built-in cathode-ray tube allowed a visual quality check of each curve prior to read out.

The MCA contents were read into an APL work space. The basic procedure adopted here was to load the device-coupler program store with the instruction necessary to read 16 channels, and to execute this device-coupler program until all 512 channels of a curve had been read into the APL work space. After completion, using a header specific for each individual curve, the next 512-point data set was read out.

B. Sample mounting and linewidth data

In all experiments a sample cut from a Verneuil-grown $SrTiO_3$ crystal doped with 0.03-wt% Fe_2O_3 was used. This crystal was delivered in 1963 by the former National Lead Company and was of good quality due to careful annealing after growth. A "monodomain" shape of $5.5 \times 1.5 \times 0.3$ mm^3 size was machined.[10] The monodomain character of this sample was roughly 95% and remained stable for several years after the initial shaping. The design of the sample holder was such that no external strain could act on the crystal during cooling down.

The mounting of the sample used in our experiments is schematically shown in Fig. 1(a). The axis of the $SrTiO_3$:Fe^{3+}-V_O center may lie along any of the crystal axes. The experiments with single-crystal samples are done with the c axis of the crystal oriented along the y axis, and the magnetic field rotated in angles θ in the x-z plane. The rf field is applied along the c axis. One can therefore observe three resonant lines corresponding to sites along the three axes. The g values for these lines shown in Fig. 1(b) correspond (a) to sites with their axis of symmetry along the z axis, (b) to sites with their axis along the x axis, and (c) to sites with their axes along the y axis.[11] Evidently sites 1 and 2 are equivalent, and we shall assume we are treating a line originating from site 1.

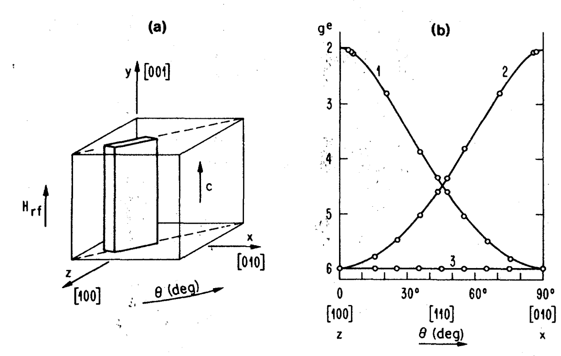

FIG. 1 (a) Sample geometry. The magnetic field was rotated in the z-x plane. (b) Anisotropy of the g values for Fe^{3+}-V_O center pointing along: 1, [100]; 2, [010]; and 3, [001].

In order to get an overview of the behavior of the linewidth of the impurity center at $T > T_c$, preliminary data were taken as a function of angle (θ:2°–80°) and temperature (T: 106–295 K) (Fig. 2).[12] In these measurements, only the peak-to-peak width was examined. In order to avoid apparent linewidth broadening, the low-frequency modulation was kept one third of the actual width of the signal. The figure clearly shows a decrease in width on lowering T to 150 K where a dramatic increase starts to take place reaching a maximum in the immediate vicinity of T_c. This increase is the evidence of the critical rotational fluctuations occurring at the antiferrodistortive phase transition.[6] The linewidth is not only temperature dependent but also depends on the angle θ in a characteristic way. At small angles, the sensitivity to the fluctuations grows rapidly until a maximum at 15° is reached, and then tails off for larger θ. A deeper understanding of these effects necessitated a better experimental resolution of the EPR signals. This was possible with the analysis of the line shape in addition to the previous peak-width determination. In the temperature range of most in-

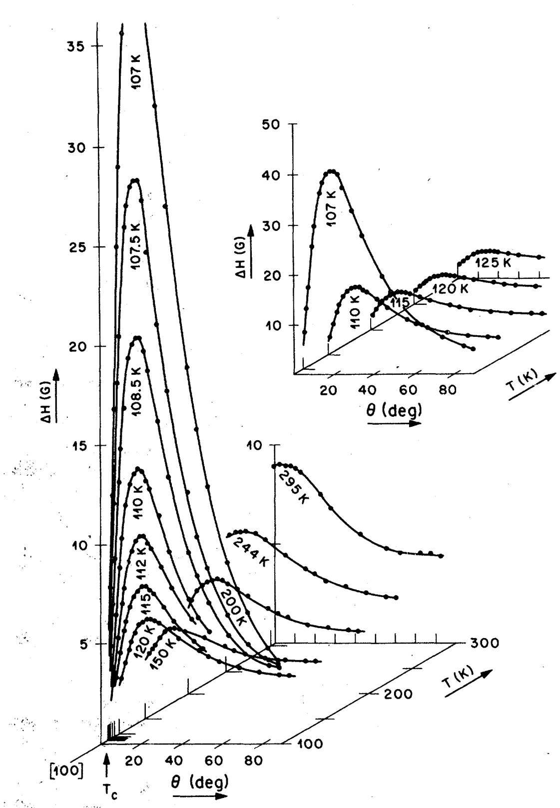

FIG. 2. Experimental linewidth as a function of angle and temperature.

terest, the former was varied in steps of 1–5 K up to 140 K. At each point, the magnetic field orientation was altered by 1° or 2° until the maximum of $\theta=15°$.

C. Line-shape data acquisition

To avoid introducing any signal shape distortion, the Zeeman modulation was always adjusted to one tenth of the measured peak-to-peak width. This ratio guarantees that line distortion is less than 1% for either Lorentzian or Gaussian line shapes.[13] The loss of signal intensity associated with the small modulation was compensated by the multiscan sequence mentioned above. From earlier measurements, we knew that above 115 K the lines are mainly of Lorentz character. Below this temperature, the Gaussian part increases.[14] Thus, during data collection the magnetic field scan was selected depending on line-shape character for maximum resolution. For more Gaussian shapes, the total sweep range was chosen to cover four times the linewidth between maximum slopes ΔH_{pp}. In the dominant Lorentz case, where the wings of the derivative curve very slowly tail off to zero, a sweep of about five to six times ΔH_{pp} was selected to include all information present in the wings.

III. THEORETICAL BACKGROUND

A. Basic equations

We will describe the Fe^{3+}-V_O complex by the spin Hamiltonian for the magnetic ion

$$H_I=g\mu_B\vec{H}\cdot\vec{S}+D(S_z^2-\tfrac{1}{4}) \ , \qquad (1)$$

where $D=1.4\,\text{cm}^{-1}$. We omit several terms of lower symmetry known to be present.[15] These produce level shifts that are at least two orders of magnitude smaller than the term we have kept, and are not necessary for analyzing the spectrum in the paramagnetic region, to the accuracy we wish to calculate. To obtain the effect of the rotation fluctuation of the oxygen octahedron (within which the Fe^{3+}-V_O centers are embedded) on the energy of the spin system, we will assume that a small rotation of the octahedron leaves the crystal field unchanged in a frame that is fixed in the octahedron. (We will later show that the fluctuations at the impurity site are proportional to those in the bulk.) With this assumption, the Hamiltonian in the rotated frame is

$$H_I'=g\mu_B\vec{H}'\cdot\vec{S}'+D(S_z'^2-\tfrac{1}{4}) \ . \qquad (2)$$

H_I' can be expressed in terms of spin operators quantized along the original axes, $\vec{H}\cdot\vec{S}=\vec{H}'\cdot\vec{S}'$, and, for rotations of angle ϕ_x about the x axis,

$$S_z'=e^{i\phi_x S_x}S_z e^{-i\phi_x S_x}=S_z+\phi_x S_y+O(\phi_x^2) \ , \qquad (3)$$

so that the effect of a small rotation is to produce a perturbation of the spin system described by

$$\begin{aligned}H_{I-L}=H_I'-H_I&=D(S_zS_y+S_yS_z)\phi_x\\&\quad-D(S_zS_x+S_xS_z)\phi_y \ . \end{aligned}\qquad (4)$$

In Eq. (4), we included the contribution from rotations about the x and y axes. Rotations about the z axis do not produce any change in the energy of the spin and hence, do not couple the lattice and spin systems. There are additional terms to be considered arising, for instance, from phonons modulating the spin environment or from distortions produced by the rotation. The former will not be critical, however, and the latter will be much smaller than the term we have kept. They will be discussed later in this section when we consider the separation of the critical contributions to the linewidth from the background due to noncritical fluctuations.

The interaction (4) is of the form treated in a general theory of motional narrowing previously developed.[16] We shall be interested first in the fast-motion limit, defined by the criterion $\Gamma_c>>\gamma$, where Γ_c is the correlation frequency of the lattice fluctuations and γ the linewidth produced by these fluctuations.

It is shown in Appendix A that the linewidth in the fast limit, measured by sweeping the frequency, is

$$\gamma=\sum_{\alpha=x,y}\sum_k{}'\,|\langle 1|O_\alpha|K\rangle|^2J_\alpha[(E_1-E_k)/\hbar]+|\langle 2|O_\alpha|K\rangle|^2J_\alpha[(E_2-E_k)/\hbar]+\sum_{\alpha=x,y}(\langle 1|O_\alpha|1\rangle-\langle 2|O_\alpha|2\rangle)^2J_\alpha(0) \ , \qquad (5)$$

where $|K\rangle$ denotes an eigenstate of the Hamiltonian (1), $O_{x,y}=D(S_zS_{y,x}+S_{y,x}S_z)$, the resonance is done between the levels $|1\rangle$ and $|2\rangle$, the prime on the summation means that the diagonal matrix elements are not included,[16] and

$$J_{x,y}(\omega)\equiv\text{Re}\int_0^\infty e^{i(\omega+i\epsilon)t}\langle\phi_{x,y}(t)\phi_{x,y}(0)\rangle\,dt \ . \qquad (6)$$

The contributions to the linewidth proportional to $J(0)$, which correspond to perturbations produced by the lattice fluctuations that modify the energy-level spacing but do not produce transitions to other levels, are called secular. The contributions arising from transitions to other levels, which depend upon the spectral density at frequencies that correspond to excitation energies of the ion system, are called nonsecular.

Due to the way in which the crystal is cut, a stress field distorts the crystal along the y axis and suppresses the fluctuations about the x axis,[10] which become noncritical although large. For the magnetic field in the x-z plane $\langle K|O_x|K\rangle$ vanishes by symmetry and only coupling to the critical fluctuations, ϕ_y, contribute to the secular width. The fluctuations about the x axis may contribute in higher order.

The spectral function $J_y(\omega)$ near $\omega=0$ is in fact the object of our interest. Neutron scattering studies, measure directly

$$J_q(\omega)\equiv \mathrm{Re}\int_0^\infty e^{i(\omega+i\epsilon)t}\langle\phi_y(q,t)\phi_y(-q,0)\rangle\,dt\ , \qquad (7)$$

where

$$\phi_y(q)=\sum_i e^{i\vec{q}\cdot\vec{r}^i}\phi_y^i\ ,$$

and ϕ_y^i is the rotation at site i. One can infer from the fact that the width of the central peak is much less than the instrumental resolution that, in these experiments, the width is less than 0.1 cm^{-1}. On the other hand, the soft-mode spectral weight is distributed smoothly over an interval of 2–3 cm^{-1}, even at T_c. The local spectral function $J(\omega)$ must look as shown in Fig. 3. This has an important consequence for the analysis of the experiment.

The frequency of the resonance is E_2-$E_1=0.645$ cm^{-1} and the frequencies of the nonsecular transition $E_{1,2}$-E_K, $K\neq 1,2$, are all higher than 1 cm^{-1}. The central peak does not contribute, therefore, to the nonsecular linewidth.

The condition $\Gamma_c >> \gamma$ has been ill defined so far. What is meant is that the spectral function $J_y(\omega)$ should vary very little over an interval γ about the frequency of the transition, and then Γ_c for a particular transition can be defined by

$$\Gamma_{c,K}^{-1}=J[(E_{1,2}-E_K)/\hbar]\Big/\int_{-\infty}^{\infty}d\omega\,J(\omega)\ . \qquad (8)$$

Since the bandwidth of the spectral function is on the order of 2 cm^{-1}, whereas γ is never more than 0.5×10^{-2} cm^{-1}, the condition that Eq. (5) be valid is

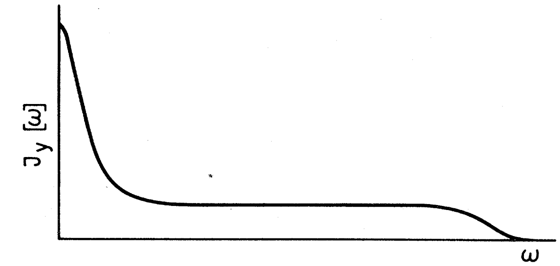

FIG. 3. Schematic behavior of spectral density $J_y(\omega)$ of local rotational fluctuations.

always well satisfied for the nonsecular transitions. This condition is not obviously satisfied for the secular transition. The width of the central peak could be smaller than the width of the resonance, and there is no conclusive evidence that the central-peak width is not zero. We want to include this possibility in the analysis. The width of the line in this case is not precisely defined since the line shape need not be Lorentzian. In general, no simple expression exists for the line shape. One can only show that the spectral function of the resonance must be of the form, to within an excellent approximation in the present case, (see Appendix B),

$$I(\omega)\propto \mathrm{Re}\,i[\omega-\omega_0-\Phi(\omega+i\gamma_{\rm NS})+i\gamma_{\rm NS}]^{-1}\ . \qquad (9)$$

Here $\omega_0=(E_2-E_1)/\hbar$ is the resonance frequency, and $\gamma_{\rm NS}$ is the nonsecular contribution to the linewidth in Eq. (5); $\Phi(\omega)$ has a perturbation expansion in powers of H_{I-L}, and involves correlation functions containing products of arbitrary numbers of $\phi_y(t)$ at different times. This result simplifies if one assumes that the fields $\phi_y(t)$ at different times t are Gaussian random variables. In this case, the spectral function depends upon the covariance $\langle\phi_y(t)\phi_y(0)\rangle$ only. It is written most simply in the time domain

$$\frac{I(t)}{I(0)}=\exp\left[-i\omega_0 t-\gamma_{\rm NS}(\theta)t-[B(\theta)]^2\times\int_0^t(t-\tau)\langle\phi_y(\tau)\phi_y(0)\rangle\,d\tau\right]\ , \qquad (9')$$

where

$$B(\theta)=\langle 1|O_y|1\rangle-\langle 2|O_y|2\rangle\ .$$

$B(\theta)$ measures the change in the angular frequency of the EPR line per unit of rotation. It may be shown that $B(\theta)$ which is by definition $(\partial\omega_0/\partial\phi_y)_{\vec{H}}$ is also $-(\partial\omega_0/\partial\theta)$. That is, a rotation of the octahedra is equivalent to a rotation of the field in the opposite direction as far as the secular terms are concerned. Here we made it explicit that the coupling coefficient between the ion and the lattice, $B(\theta)$, depends upon the angle of the field with respect to the crystal axis, as does the damping due to the nonsecular terms, $\gamma_{\rm NS}(\theta)$. This expression, without the $\gamma_{\rm NS}(\theta)$ damping, was derived previously by Kubo and Tomita.[17] An alternate informative way of writing Eq. (9′) is

$$\frac{I(t)}{I(0)}=\exp\left[-i\omega_0 t-\gamma_{\rm NS}(\theta)t-[B(\theta)]^2\frac{2}{\pi}\times\int_{-\infty}^{\infty}J_y(\omega)\frac{\sin^2(\omega t/2)}{\omega^2}\,d\omega\right]\ . \qquad (10)$$

An elementary derivation of the secular contribution to Eq. (10) is given in Appendix C. Equation (10) may also be obtained direct from Eq. (9′).

B. Fast- and slow-motion regimes

For sufficiently long times ($t > 1/\Gamma_c$) such that $J_y(\omega)$ does not vary significantly on a frequency scale of $1/t$, we may regard the factor of $[\sin^2\frac{1}{2}(\omega t)]/\omega^2$ as a delta function of weight $\frac{1}{2}(t\pi)$, and we obtain the result (5) for the total linewidth.

Consider however the opposite limit, that $J(\omega)=\pi\delta(\omega)$, i.e., the fluctuations are completely static, then

$$\frac{I(t)}{I(0)}=\exp\{-i\omega_0 t-\gamma_{\rm NS}(\theta)t-[B(\theta)t]^2/2\} \ . \tag{11}$$

The line is now Gaussian, with a width $B(\theta)$. Note that in the passage from the fast limit $\Gamma_c >> \gamma$ to the slow limit $\Gamma_c << \gamma$, the linewidth γ_S resulting from the secular fluctuations, changes from being proportional to $[B(\theta)]^2$ to being proportional to $B(\theta)$, while the line shape changes from Lorentzian to Gaussian.

That the line shape should be Gaussian in the slow limit is a consequence of the assumption of Gaussian statistics for the fluctuations ϕ, but the dependence on the coupling constant in the two limits is an exact general result. To see this, observe that if the fields ϕ are static, then for any fixed value ϕ_0, the frequency of the resonance is shifted to

$$\omega=\omega_0+(\langle 1|O_y|1\rangle-\langle 2|O_y|2\rangle)\phi_0 \ . \tag{12}$$

The spectral function for this field value, neglecting for the moment $\gamma_{\rm NS}$, is

$$I_0(\omega)=I_0(t=0)\delta(\omega-\omega_0-B(\theta)\phi_0) \ . \tag{13}$$

Since we must average over field values with a distribution $P(\phi)$, the measured response is

$$I(\omega)=\frac{I(t=0)}{B(\theta)}P\left[\frac{\omega-\omega_0}{B(\theta)}\right] \ . \tag{14}$$

The line shape is then a direct measure of the $P(\theta)$ and the width is proportional to $B(\theta)$. If we include the nonsecular terms, then

$$I(\omega)=I(t=0)P\left[\frac{\omega-\omega_0}{B(\theta)}\right]*\frac{1}{\pi}$$
$$\times\gamma_{\rm NS}\Big/[(\omega-\omega_0)^2+\gamma_{\rm NS}^2] \ , \tag{15}$$

where the asterisk indicates a convolution.

We therefore have two unequivocal results in the fast and slow limits. If the fast limit holds, $\gamma_S\propto B(\theta)^2$ and the line shape must be Lorentzian, with a width $\gamma_S+\gamma_{\rm NS}$, while if the fluctuations responsible for the central peak are completely static, then $\gamma_S\propto B(\theta)$ and the line shape is the convolution of the probability distribution of the fields with a Lorentzian whose width is $\gamma_{\rm NS}(\theta)$. Hence, knowing $\gamma_{\rm NS}(\theta)$ and $B(\theta)$ can provide an unambiguous way of deciding which situation holds. Note that the line shape can be Lorentzian even in the slow limit, if only $P(\phi)$ is Lorentzian, so that this fact alone does not enable one to decide which situation holds. In fact, as we shall see later, a model in which the central peak is due entirely to impurities producing a static distribution of fields ϕ can produce a changeover in line shape from Lorentzian to approximately Gaussian, as the temperature approaches T_c, just as in the case of a dynamical crossover from the fast to the slow regime. The only unambiguous determination of whether the line is due to fast or slow fluctuations is a determination of the dependence of the linewidth on $B(\theta)$. This has also been pointed out by Folk and Schwabl.[14]

C. Evaluation of matrix elements

$B(\theta)$ and the matrix elements needed to calculate $\gamma_{\rm NS}(\theta)$, may be readily obtained from the Hamiltonian (1) and the definition of the operator O_y contained in Eq. (4). This procedure is complicated somewhat by the fact that the linewidth measurements are made at a constant frequency, by sweeping the field. The frequency of the resonance $\omega=(E_2-E_1)/\hbar$ is fixed at 0.645 cm^{-1}. The value of the field at resonance necessary to produce this splitting depends on angle. Hence, in order to obtain the matrix elements, the Hamiltonian (1) is diagonalized with a value of H previously found to give the correct splitting at the angle chosen. The operators in Eq. (4) are transformed to this basis and the matrix elements read out.

In order to calculate $\gamma_{\rm NS}(\theta)$, the function $J_y(\omega)$ must be known for many values of ω. These are all within a range in which the spectral function may be assumed as slowly varying (this is the case for two-dimensional simulations[18] but ought to be better in three dimensions), and all equal. In fact, one matrix element dominates the sum in Eq. (4) and hence the angular dependence of $\gamma_{\rm NS}(\theta)$ does not depend sensitively on this assumption. The angular dependence of the secular linewidth $\gamma_S(\theta)$ is known precisely with no ambiguity, since it depends on only a single matrix element.

D. Field-swept linewidth

Let us define an effective g value by

$$(E_2-E_1)/\hbar=\omega_0=\mu_B g(H,\theta)H\equiv G(H,\theta)H \ . \tag{16}$$

The values of $G(H,\theta)$ obtained by diagonalizing the full Hamiltonian are in agreement to better than 1%

with those obtained previously by perturbation methods.[15] $E_{1,2}$ are the energy levels appropriate to applying H at an angle θ from the quantization axis (z axis). At resonance, $\omega_0 = \omega_{\text{res}} \equiv 0.645\ \text{cm}^{-1}$. Let us define a field H_R so that

$$G(H_R, \theta) H_R = 0.645\ \text{cm}^{-1} \ . \tag{17}$$

Then the magnitude of the variable

$$\delta\omega \equiv \omega_{\text{res}} - \omega_0 \tag{18}$$

is

$$\delta\omega \equiv \left[G(H_R, \theta) + \frac{\partial G}{\partial H}(H_R, \theta) H_R \right] \delta H \ , \tag{19}$$

where $\delta H = H_R - H$. Equation (19) expresses the relation between the experimentally measured changes in δH and the theoretical expressions in terms of $\delta\omega$. In the fast regime, where $\Phi(\omega)$ does not depend sensitively on ω over an interval of size comparable to the linewidth, we would have for the intensity of the observed signal

$$\frac{I(H)}{I(t=0)} = \text{Re} \left[\frac{i}{\delta\omega + i[\gamma(\theta) + \gamma_{\text{NS}}(\theta)]} \right] = \text{Re} \left[\frac{i}{[G(H_R, \theta) + \frac{dG}{dH}(H_R, \theta) H_R] \delta H + i[\gamma(\theta) + \gamma_{\text{NS}}(\theta)]} \right] \ . \tag{20}$$

The observed line shape is Lorentzian, with a half-width

$$\gamma_H(\theta) = [\gamma_{\text{S}}(\theta) + \gamma_{\text{NS}}(\theta)] \left[G(H_R, \theta) + \frac{dG}{dH}(H_R, \theta) H_R \right]^{-1} \ . \tag{21}$$

The factor $(dG/dH) H_R$ is only about 1% of $G(H, \theta)$ and does not significantly affect our results. For the sake of brevity we will neglect it.

More generally, we would have

$$I(H) \propto \text{Re}\, i \{ \Delta H + [\phi(\Delta H G(H_R, \theta)) + i \gamma_{\text{NS}}(\theta)] / G(H_R, \theta) \}^{-1} \ . \tag{22}$$

In the slow limit, this result simplifies again,

$$I(H) \propto P \left[\frac{G(H_R, \theta)}{B(\theta)} \Delta H \right] * \frac{1}{\pi} \frac{\gamma_{\text{NS}}(\theta)/G(H_R, \theta)}{\{\Delta H^2 + [\gamma_{\text{NS}}(\theta)/G(H_R, \theta)]^2\}} \ . \tag{23}$$

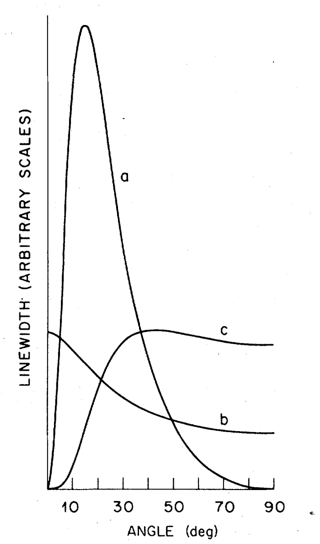

FIG. 4. Theoretical dependence of the contributions to the linewidth ΔH on angle θ between crystal axes: a, $\Delta H_S^S(\theta) = A(\theta) = B(\theta)/G(\theta)$, note the resemblance to the 107-K data (Fig. 2); b, $\Delta H_{\text{NS}}^F(\theta) = \gamma_{\text{NS}}(\theta)/G(\theta)$, note the resemblance to the 295 K data in Fig. 2; and c, quadratic contribution to the linewidth.

We show, in Fig. 4, the variation of the field-swept linewidth with angle, for the secular and nonsecular terms, assuming both are in the fast regime. The angular dependence of the nonsecular linewidth is due almost entirely to the variation of $G(H, \theta)$ with angle. The scales are arbitrary, the actual linewidths depending upon $J_y(\omega)$.

E. Other contributions to the linewidth

Inspection of the data reveals that there must be additional contributions to the linewidth not included so far, since the linewidth at $\theta = 0°$ must be about three times that at $\theta = 90°$ if only γ_{S} and γ_{NS} are considered, and this is not observed. The additional linewidth is not large (about 1 G) and our results do not hinge on knowing its origin. Some hypothesis about its angular dependence must be made if we are to include it in a fit to the linewidth data as a function of angle, and we have considered several mechanisms.

(i) The contribution from the second-order terms due to the rotations. These yield a Hamiltonian $\phi_y^2(S_x^2 - S_x^2) + \phi_x^2(S_z^2 - S_y^2)$, and give for the corresponding secular and nonsecular terms the angular variation shown in Fig. 4(c). Note that the are not expected to show large increases in the critical region since the spectral density for $\langle\phi^2(t)\phi^2(0)\rangle$ should be noncritical. (ii) The contribution from the hyperfine coupling to the iron nuclei or adjacent nuclei is of the form $\vec{I}\cdot\vec{S}$. This leads to an inhomogeneous broadening of the line since the nuclear spins can be regarded as static on the time scale of the electronic decay, and there is no nonsecular contribution. The resultant linewidth is independent of angle in the present case and noncritical. (iii) The effect of phonon modulations of the crystal-field environment. The simplest term would be proportional to S_z^2. No critical effects would be expected due to such terms and since the nonsecular line shape is essentially the same as that due to the rotation fluctuations, they will not be considered further.

F. Summary

The fluctuations of the orientation of the lattice octahedra containing the Fe^{3+}-V_O impurity broaden the EPR resonance line. The broadening may be classified as nonsecular or secular, depending upon whether the fluctuations induce a transition in the ion (nonsecular) or not. The nonsecular contribution to the linewidth arises from lattice vibrations whose frequency is of the order of 2 cm^{-1}, or larger. These are assumed to be in the fast regime with a characteristic decay frequency much greater than the observed linewidth. The nonsecular linewidth will not be affected by the presence of the central peak and is expected to be noncritical.

The secular contribution arises from fluctuations with frequency near zero, contains the contribution from the central peak and is expected to show a critical increase.

Two situations are to be distinguished. (a) The width of the central peak is much greater than the width of the observed EPR resonance. In this case, the secular broadening is said to be in the fast regime. The line shape must be Lorentzian and the linewidth, measured by varying H, is proportional to $B(\theta)^2/G(H_R,\theta)$. (b) The central peak is static or has a width much less than that of the observed resonance. The line shape is determined by the probability distribution of the local fields, and the linewidth is proportional to $B(\theta)/G(H,\theta)$. Intermediate cases are possible but it is only in the two limiting situations that the linewidth has an unambiguous dependence upon angle.

There is a small additional noncritical contribution to the linewidth, due perhaps to hyperfine coupling, second-order effects of the rotations, or phonon modulations.

In Sec. IV, we shall analyze the angular dependence of the linewidth and show unequivocally that the secular fluctuations are always slow for the range of temperatures in which they are observable, obtaining in this way an upper limit on the width of the central peak and a measurement of the distribution function for local fluctuations.

IV. ANALYSIS OF DATA

The linewidth as a function of angle and temperature is shown in Fig. 2. A comparison of the figure with the angular variations due to the secular and nonsecular terms (Fig. 4) indicates immediately that there is a dramatic increase in the secular component of the linewidth as $T\to T_c$. [The linewidth is defined to be half the distance between the maximum and minimum of $dI(H)/dH$.] We fitted the data at each temperature to an assumed form

$$\Delta H(\theta)=A_1\Delta H_S^F(\theta)+A_2\Delta H_{NS}(\theta)+A_3\Delta H_r(\theta)\ , \tag{24}$$

where

$$\Delta H_S^F(\theta)=\frac{B(\theta)^2}{G(H_R,\theta)},\quad \Delta H_{NS}(\theta)=\frac{\gamma_{NS}(\theta)}{G(H_R,\theta)}\ ,$$

and $\Delta H_r(\theta)$ is a residual linewidth assumed to arise from one of the sources mentioned in Sec. I E.

For $\Delta H_r(\theta)$, we used both the result one obtains for inhomogeneous hyperfine broadening and that for secular second-order rotation fluctuations, the latter being calculated for both slow and fast regimes. The hyperfine coupling gives unphysical negative values for A_2, and large values for A_3. The best fits are obtained using slow second-order rotation fluctuations. We shall use this assumed form for $\Delta H_r(\theta)$ in all the subsequent analysis. None of our conclusions hinges on this being the correct mechanism for the residual linewidth, which is at most ≈ 1 G in all cases.

We also fitted the data using

$$\Delta H(\theta)=A_1^1\,\Delta H_S^S(\theta)+A_2^1\,\Delta H_{NS}(\theta)+A_3^1\,\Delta H_r(\theta)\ , \tag{25}$$

where $\Delta H_S^S(\theta)$ is the secular linewidth in the slow regime, $B(\theta)/G(H_R,\theta)$. If the line shape is not Lorentzian, the half-width cannot be obtained by simply adding the various contributions and, indeed, the line shape changes with angle. However, the corrections needed to incorporate this effect are small, this form for the half-width being adequate for the moment. In Fig. 5, we show the data fit by both forms for $\Delta H(\theta)$, at a temperature of 107 K or ≈ 1.5 K above the transition. It is evident from a visual inspection that the assumption of slow, secular contributions to the linewidth gives a better fit to the data than the assumption that the secular contributions are fast. This is borne out by the value for the least squares in each case which is shown as a function of temperature in Fig. 6. The fit with the slow

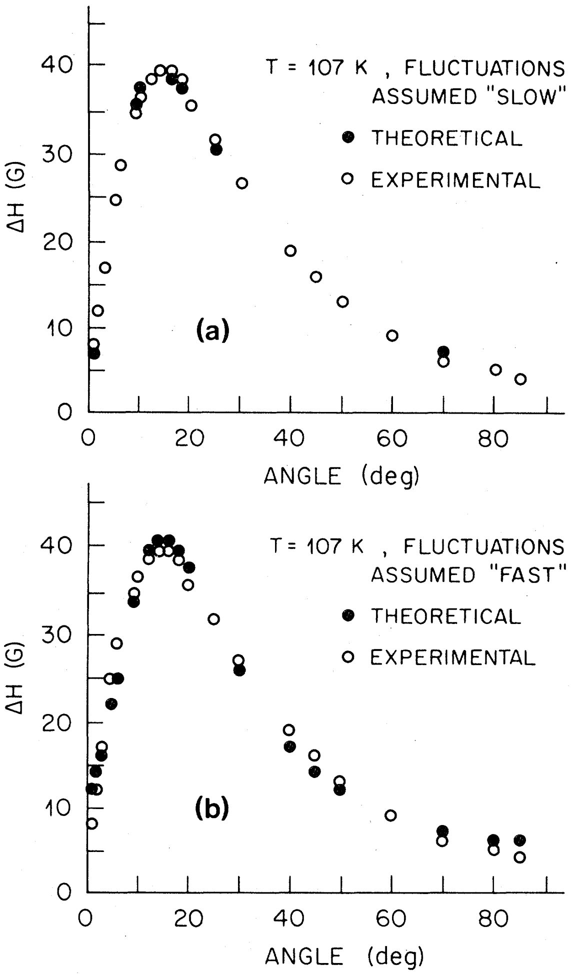

FIG. 5. Comparison of measured and calculated peak-to-peak linewidths ΔH_{pp} as a function of angle θ between $\vec{H}$ and $\hat{z}$ for (a) slow- and (b) fast-motion regimes.

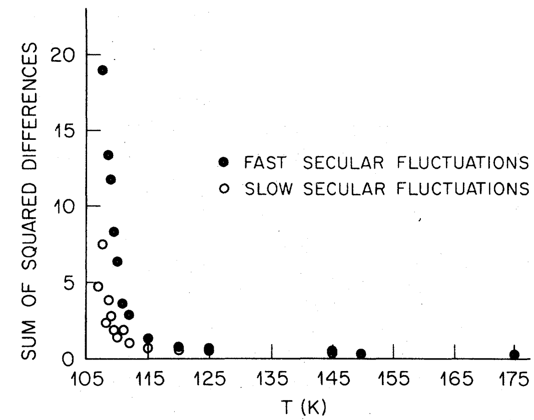

FIG. 6. Relative sum of squared differences for least-square fits of angular dependencies of measured and theoretical form (Fig. 5) for slow- and fast-motion regimes as a function of temperature.

linewidth is clearly significantly better than that with fast linewidths near T_c, although the significance of the difference is questionable at temperatures above 120 K. Using the slow linewidths, in Fig. 7 we showed the contribution from the secular fluctuations $A_1^1\,\Delta H_S^S(\theta)$, the nonsecular fluctuations $A_2^1\,\Delta H_{NS}(\theta)$ and the residual linewidth at an angle of 14° where the secular terms are almost their maximum value, relative to the remainder, giving the maximum sensitivity for observing the effects of the lattice fluctuations at or near $\omega=0$. As was expected, the secular linewidth shows a critical increase, whereas the nonsecular and residual terms do not. (Earlier work[12] in which an apparent critical increase in the nonsecular linewidth was reported, was incorrect due to a mistake in the fitting program.)

In order to discriminate between the two extreme hypotheses with greater sensitivity, we will now consider only the small-angle data, i.e., the data between 0° and 15°. The primary advantage of this is that it makes the background subtraction, i.e., the separation of $\Delta H_{NS}(\theta)$ and $\Delta H_r(\theta)$ from $\Delta H(\theta)$, less ambiguous. $\Delta H_{NS}(\theta)$ is almost independent of angle in this range, and the combination of $\Delta H_{NS}(\theta)$ and $\Delta H_r(\theta)$ even more so (see Fig. 4). Any additional background terms from unexamined sources which must have a small amplitude in any case (< 1 G), would be unlikely to have significant variation over this small range of angles. $G(H_R,\theta)$ is also almost constant, so that the fast linewidth is proportional to $B(\theta)^2/G(\theta)$, whereas the slow one is proportional to $B(\theta)/G(\theta)$. Since $B(\theta)$ vanishes at $\theta=0$ and achieves its maximum near 15°, we do not lose any sensitivity in restricting the angular variation to this range.

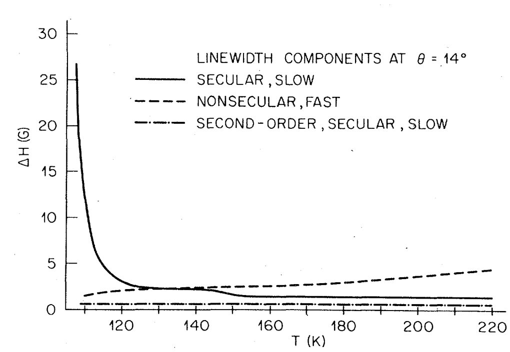

FIG. 7. Contributions to observed linewidth at $\theta=14°$ from $\Delta H_S^S(\theta)$ secular slow, $\Delta H_{NS}^F(\theta)$ nonsecular fast, and $\Delta H_S^S(\theta)$ second-order secular slow.

The results for the same data as fitted previously is shown in Figs. 8 and 9. The result is unambiguous. If the assumption of fast linewidths were correct, which would be best for small values of $B(\theta)$, then the line shape would be Lorentzian and the incremental linewidth above the background would be proportional to $B(\theta)^2/G(H_R,\theta)$, giving a linear fit to Fig. 8. No such fit is possible for the data up to 115 K and the attempt to impose such a fit leads to a background at 0° which must be changing dramatically in the temperature range 109 to 115 K, in contradiction to our expectations and the results of the previous analysis of the data (Fig. 7). The assumption of a slow linewidth, on the other hand, leads to a rather good fit to the data and an extrapolated background that does not show any significant temperature variation. (It is not possible to measure the linewidth at 0° due to the interference with a line arising from sites with a different orientation in the crystal.) We conclude that below 115 K our results are consistent with the assumption that the central peak is completely static. As will be seen, the resolution of the experiment is set by the background linewidth of ≈ 2 G, so that we have an upper limit of 2 G $\approx$ 6 MHz on the possible width of the fluctuations in the local order parameter, i.e., the width of a peak in $J_y(\omega)$ near $\omega=0$. The width of the peak in $J_q(\omega)$ at the zone corner must be even smaller.[14]

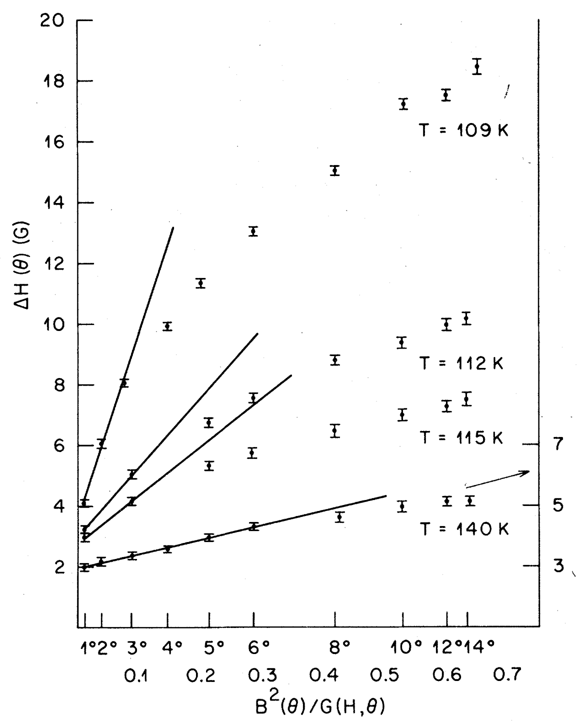

FIG. 8. Measured $\Delta H(\theta)$ linewidth vs $\Delta H_S^f = B^2(\theta)/G(\theta)$, for various temperatures, should be linear if fast-motion regime holds.

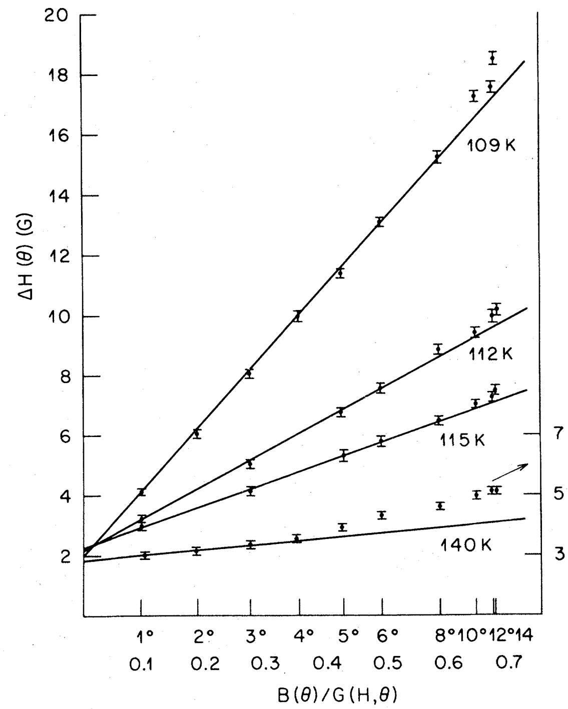

FIG. 9. Measured $\Delta H(\theta)$ linewidth vs $\Delta H_S^s = B(\theta)/G(\theta)$ for various temperatures is linear if slow-motion regime holds.

We note that line shapes are almost Lorentzian at 115 K, even at the largest angles becoming Gaussian at about 107.5 K, and flatter than Gaussian below that. As mentioned previously, this alone does not contradict the conclusion that the fluctuations responsible for the broadening are static and we shall show in Sec. V, that a model based upon static fluctuations due to point impurities can indeed produce just such a crossover in line shape. Failure to appreciate this possibility, together with limited data on the dependence of the linewidth on the coupling parameter $B(\theta)$, led us earlier to the incorrect conclusion that the crossover in line shape was of dynamic origin.[12,14]

The data at 140 K is inconclusive and is equally well fitted either way. In order to test the possibility that a dynamical crossover does occur above 115 K, additional measurements were made in the small-angle range for temperatures from 117 to 143 K. In this range, the maximum increase in the linewidth due to the secular contribution is comparable to the background and diminishes with temperature so that the sensitivity of the experiment is deteriorating. It would nevertheless be possible to distinguish between the two cases if a dynamical crossover did occur.

In order to test the limits of sensitivity of the experiment in the presence of nonsecular relaxation γ_{NS}, we generated linewidth data as a function of coupling parameter for a range of values of the correlation frequency $\Gamma_c \equiv 1/\tau_0$. In Eq. (10), if we scale the frequency so that $\gamma_{\rm NS}=1$, and assume $\langle \phi_y(t)\phi_y(0)\rangle = e^{-t/t_0}$, we obtain the results shown in Fig. 10 for the linewidth as a function of the coupling strength $[B(\theta)]^2$. It is clear from Fig. 10 that if a crossover did exist, i.e., the frequency $1/t_0$ went from being one quarter of to four times more than the observed minimum width, the departures from linearity on a plot of linewidth versus $[B(\theta)]^2$ would be notable. This is the case even if the range of coupling constants were such that the linewidth increased by no more than a factor of 2 from its minimum value, as observed at high temperatures. The resolution of the experiment is therefore on the order of the minimum linewidth of 2 G.

Some indication that a crossover might be present is indicated in the data at 123 K. In Figs. 11 and 12, we show the data fit to a straight line on a plot of linewidth versus $B(\theta)/G(H_R,\theta)$ and versus $[B(\theta)]^2/G(H_R,\theta)$. The changes in the line shape with coupling strength can produce very little difference in the numerical factor relating $B(\theta)$ and the linewidth in the slow limit, so that the straight line should describe the data in Fig. 11 if the fluctuations are static. The two fits to the data are equally good. Above 123 K, the results are equally inconclusive. The data at 117 K are clearly slow. We conclude therefore that the width of the local fluctuations Γ_c, is less than the resolution set by the background, 2 G or $\simeq 6$ MHz for temperatures up to 117 K or $T_c + 11$ K.

Since this is the case, the data is entirely in the slow regime and provides a measurement of $P(\phi)$ the probability distribution for the local value of the order parameter. We cannot, of course, rule out a

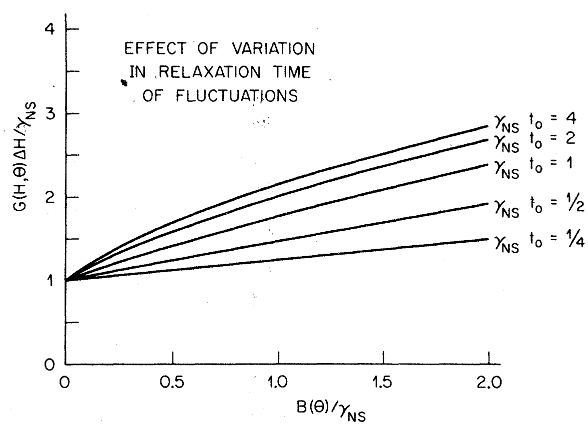

FIG. 10. Calculated linewidth (between derivative extrema) divided by that produced by the nonsecular terms alone. Calculation assumes a Lorentzian-model local-fluctuation spectrum of half-width $\gamma_l = t_0^{-1}$. Parameter labeling for the different curves is $\gamma_{\rm NS} t_0$.

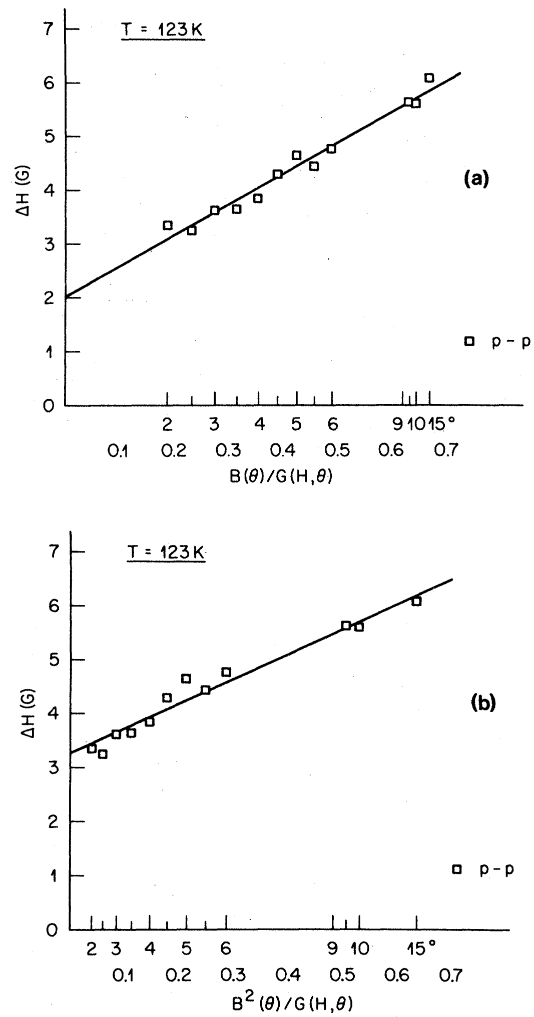

FIG. 11. Linewidth data at 123 K, fitted using Eq. (26) for (a) slow- and (b) fast-motion regimes.

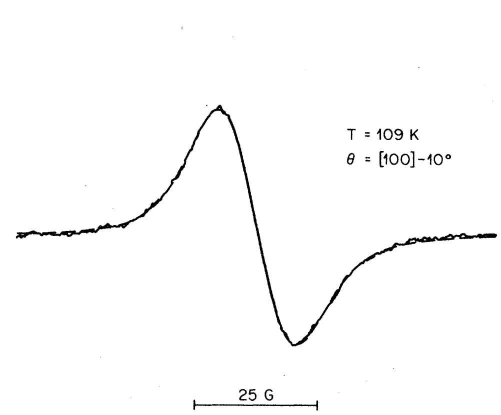

FIG. 12. Fitted derivation of EPR line at $T=109$ K at $\theta=[100]-10°$.

dynamical width much smaller than 2 G, which will have the effect of introducing an additional resolution function into the measurement, but since this is a sufficiently small width, it can be neglected, if present, particularly near the transition.

Recently, linewidth measurements $\Delta H(T)$ at 9.2 GHz on the same sample confirmed the present analysis: The measurements were carried out at an angle $\theta=45°$ ($\vec{H}\parallel[110]$)[19]: The critical secular contribution was found to scale with the frequency. This is inevitable if the width results from the slow-motion regime and is proportional to $B(\theta)/G(\theta H)=A(\theta)$. Now $B(\theta)=\partial\omega_0/\partial\theta=[\partial G(H,\theta)/\partial\theta]H$. As $G(\theta,H)$ and $\partial G(\theta,H)/\partial\theta$ change by a few percent when going from $\omega=19.4$ GHz to 9.2 GHz, ΔH scales with the resonance field H, i.e., with ω as observed. On the other hand, the nonsecular linewidth is proportional to the local spectral density $J(\omega)$, with ω being the difference of the ground-state spin levels $|1\rangle$ and $|2\rangle$ to the existing levels of the Fe^{3+}-V_O impurity located at 2.8 and 5.6 cm^{-1}, respectively. As $J(\omega)$ was assumed flat in that range, ΔH_{NS} is not expected to change if the ground-state splitting is reduced from 0.645 cm^{-1} (19.4 GHz) to 0.33 cm^{-1} (9.2 GHz). This independence of ΔH_{NS} to ω is also borne out by the experiment.

In order to fit the data, we have assumed that the line shape is the Fourier transform of

$$e^{-\Gamma_1 t-(\Gamma_2 t)^2/2}\ , \tag{26}$$

i.e., the convolution of a Lorentzian and a Gaussian. The line shape has been fitted for angles between 0° and 14°, and Γ_1 and Γ_2 obtained as a function of $B(\theta)$ for temperatures from 107 to 143 K. There is no particular justification for the form (26) other than that it is the beginning of a cumulant expansion of the relaxation function. However, the fits to the data are satisfactory (see Fig. 12 for a typical fit) and the line shape is adequately summarized by Γ_1 and Γ_2. The least-square fits also fit the line center, intensity, and asymmetry (due to measuring bridge imbalance) of the line. The measurements below 107 K cannot be fitted this way as the line shapes are more localized at low frequencies than a Gaussian. We will present this data separately.

Γ_1 and Γ_2 vary linearly with $B(\theta)$, which makes it possible to subtract the background. There is about half a Gauss of Gaussian background that cannot be accounted for perhaps due to hyperfine effects, and we have subtracted this from the value of Γ_2 assuming it is constant with angle. The Lorentzian background has also been assumed constant with angle. In Fig. 13, we show $\Gamma_1/B(\theta)$ and $\Gamma_2/B(\theta)$ for $\theta=14°$, with the background subtractions made as a function of temperature. In Fig. 14, we show the actual line shape for $T=106$ K, which corresponds to $T_c+0.4$ K in this sample. The results of Figs. 13 and

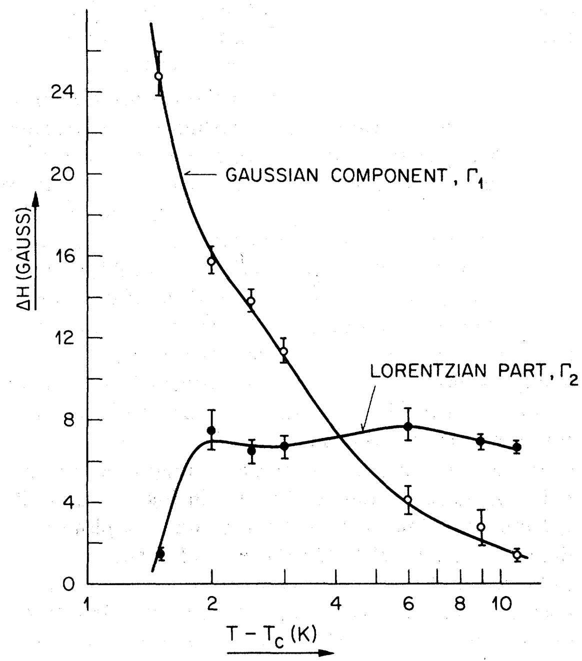

FIG. 13. Variation of Lorentzian (Γ_1) and Gaussian (Γ_2) components of the line shape as a function of temperature. The background, i.e., values of Γ_1, Γ_2 at $\theta=0$ has been subtracted. The probability distribution of local fields is related to Γ_1 and Γ_2 by

$$p(\phi)\propto\int_{-\infty}^{\infty}e^{i\phi x}e^{-\Gamma_1' x-(\Gamma_2' x)^2/2}dx\ ,$$

where

$$\Gamma_1'=A^{-1}(\theta)\Gamma_1,\quad \Gamma_2'=A^{-1}(\theta)\Gamma_2\ ,$$

and $A(\theta)$ takes its maximum value of 9.7×10^{10} sec^{-1}/rad.

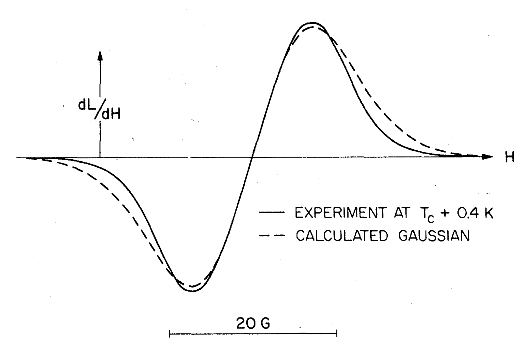

FIG. 14. Comparison of experimental EPR-line derivative dL/dH at $T_c+0.4$ K with a Gaussian fitted to the slope at $H=H_0$.

14 give an absolute measurement of the probability distribution of the fluctuations in the local order parameter, $\delta\phi_y$, and provide a test for future theories of the transition.[20]

One may argue that the Fe^{3+}-V_O center does not reflect the rotation of intrinsic TiO_6 octahedra. However, the rotation angle $\langle\phi(T)\rangle$ observed with this center below T_c is exactly proportional to the order parameter $\langle\phi(T)\rangle$ as measured by the Fe^{3+} center on a Ti site without an oxygen vacancy, with $\langle\phi(T)\rangle = 1.59\langle\bar{\phi}(T)\rangle$ in a temperature range of 30 K.[21] The linearity shows that $\langle\bar{\phi}(T)\rangle$ is not center dependent. One can conclude that $\bar{\phi}$ itself is also proportional to the bulk value of ϕ as any nonlinearities would be reflected in different temperature dependencies of $\langle\phi(T)\rangle$ and $\langle\bar{\phi}(T)\rangle$. Therefore, this center certainly shows the static average rotation angle correctly below T_c. Above T_c there might be a difference if the critical linewidth increase were dynamic in origin because in the Fe^{3+}-V_O center an oxygen is missing and the moment of inertia is lower. But we have shown that the critical increase of the linewidth above T_c is entirely static in character. Thus the line shape reflects the probability distribution $P(\phi)$ above T_c.

V. INTERPRETATION AND DISCUSSION

A. Static impurity model

The crossover from Lorentzian to Gaussian line shapes was previously interpreted as a dynamical crossover.[14] We show here that a model in which the fluctuations are due to static strains resulting from frozen-in impurities can also explain qualitatively the main features of the data. We shall assume that there are impurities present that couple linearly to the order parameter, the rotation angle of the octahedra, by producing a stress field in the crystal. We will then take the rotation $\delta\phi(r)$ at the site r' to be

$$\delta\phi(r-r') = \int \chi(r-r'')\psi(r''-r')\,d^3r'' \ , \tag{27}$$

where ψ is an effective stress field, and χ is an appropriate susceptibility. That is, we shall assume that the rotation may be calculated from the linear response theory. We will examine this assumption further later. There will be a large number of impurities distributed at random positions in the crystal ("quenched impurities"), and we will further assume that the total fluctuation produced by these impurities is the sum of the individual contributions

$$\delta\phi(r) = \sum_{i=1}^{N} \int \chi(r-r'')\psi(r''-r_i)\,d^3r'' \ , \tag{28}$$

i.e., the impurities do not interact.

The problem of calculating $P(\delta\phi)$ the probability distribution of the field fluctuations, has been solved in this context by Stoneham.[22] In the limit that $N\rightarrow\infty$

$$P(\delta\phi) = \frac{1}{2\pi}\int dx\, e^{ix\delta\phi}e^{-\rho H(x)} \ . \tag{29}$$

Here, $\rho = N/V$ where V is the volume of the crystal, ρ is the density of impurities, and

$$H(x) = \int dz\, p(z)(1-e^{-ix\delta\phi(z)}) \ . \tag{30}$$

$p(z) = 4\pi z^2$ if the impurities are distributed at random, as assumed, and $\delta\phi(z)$ is the rotation produced by a single impurity a distance z from the site under consideration. For the sake of simplicity, we have omitted all angular variations due to the orientation of the axis joining the impurities with the crystal axis, as they do not affect our argument. The imaginary part of $H(x)$ produces only a frequency shift, the real part being

$$\begin{aligned}\mathrm{Re}H(x) &= \int dz\, p(z)[1-\cos x\,\delta\phi(z)] \\ &= 2\int dz\, p(z)\sin^2[x\,\delta\phi(z)] \\ &= 2\int (\delta\phi)^2 p(z(\delta\phi))\frac{dz(\delta\phi)}{d\delta\phi} \\ &\quad\times \frac{\sin^2(x\delta\phi/2)}{(\delta\phi)^2}d\delta\phi \ .\end{aligned} \tag{31}$$

Here $z(\delta\phi)$ is the inverse function of $\delta\phi(z)$ which is a monotonic function of z. Defining

$$J'(\omega) = \rho\pi\omega^2 p(z(\omega))\frac{dz(\omega)}{d\omega} \tag{32}$$

we see that the distribution of the local value of the order parameter is

$$p(\delta\phi) = \frac{1}{2\pi}\int e^{ix\delta\phi}\exp\left[-(2/\pi)\int J'(\omega)\frac{\sin^2(\omega x/2)}{\omega^2}\,d\omega\right] \ . \tag{33}$$

The actual line shape, as in Eq. (15), will be the convolution of this function, appropriately scaled, with the Lorentzian arising from the nonsecular damping, i.e.,

$$\frac{I(\omega)}{I(t=0)} = \frac{1}{2\pi}\int e^{+i\omega x}f(x)\,dx \ , \tag{34}$$

where

$$f(x)=\exp\left[-i\omega_0 x-\gamma_{\rm NS}x-(2/\pi)B(\theta)\int_{-\infty}^{\infty}J'\left[\frac{\omega}{B(\theta)}\right]\frac{\sin^2(\omega x/2)}{\omega^2}\,d\omega\right] . \tag{35}$$

The resemblance to Eq. (10) should be noted, making it apparent that a line shape arising from dynamical effects may also result from static strains. We may apply the same considerations for determining the line shape due to $J'(\omega)$ as applied previously to $J(\omega)$. In particular, if $J'(\omega)$ is independent of frequency over a range of frequencies much greater than the linewidth, the line will be Lorentzian. For temperatures higher than T_c, where the coherence length is much less than the distance between impurities, $\chi(r-r')\approx\chi_0\delta(r-r')$, and

$$\delta\phi(r-r')\approx\chi_0\psi(r-r') .$$

In the continuum approximation, the stress produced by a point defect would fall off as $1/r^3$. Let us assume that this is the case for $\psi(r)$, then

$$\delta\phi(z)\propto\chi_0/z^3,\quad z(\omega)=(\chi_0^{-1}\omega)^{-1/3}$$

and

$$J'(\omega)=\omega^2\pi(\chi_0^{-1}\omega)^{-2/3}\times\tfrac{1}{3}\chi_0^{+1/3}\omega^{-4/3}=\tfrac{1}{3}\pi\chi_0 ,$$

i.e., the line shape will be Lorentzian. As the coherence length increases, a progressively larger volume around the impurity will contribute to total strain, and the effective value of χ_0 as well as the linewidth will increase. The line shape will remain Lorentzian until one is sufficiently close to the critical point that the spatial dependence of $\chi(r)$, rather than $\psi(r)$, determines $\delta\phi(z)$. At T_c, we might assume $\delta\phi\sim 1/z$, which yields a divergent linewidth. This is not observed and, in fact, cannot be expected to hold since the impurities will begin to interact when the coherence length is equal to the interimpurity spacing, violating the assumption that the field at one point is the sum of the contributions from all the impurities treated as though they were evaluated independently of one another. Nevertheless, the trend toward lower frequencies being emphasized in $J'(\omega)$ as the coherence length increases will be correct, and we expect that $J'(\omega)$ will begin to look rather like Fig. 3, the line shape tending towards Gaussian, as observed. In fact, the line shape is flatter than Gaussian at temperatures below 107 K and above 106 K, the transition temperature. It remains an open problem to provide a description of the effect of impurities on the local fields near T_c.

B. Possible interpretations

We have seen that the assumption that the central peak is the result of scattering from a distribution of static strains in the crystal due to point impurities, gives a satisfactory qualitative description of the data. As pointed out by Axe *et al.*[23] this explanation also suffices to account for the neutron scattering data in the absence of any resolved width. It is not necessary, however, that the impurities be purely static. They may in fact have some motion associated with them, as long as its characteristic frequency is $\ll 6$ MHz. There is, in fact, evidence from other experiments that this is so. Müller *et al.*[24] have observed a changeover for a resonance pattern [for Cr^{5+} ions in KDP (KH_2PO_4)] from a high- to a low-temperature configuration, characteristic of the ordered phase, at a temperature much above the transition temperature. The natural explanation for this is that regions around the EPR center are "stuck" in one or the other of the ordered configurations for a time long compared to the EPR lifetime. A theoretical treatment of this phenomenon has been given by Höck and Thomas,[25] who showed that within the context of mean-field theory, an impurity that produces a local mode below the soft-mode band will cause a local condensation at some temperature $T^*>T_c$, at which the local mode extends a distance of the coherence length. That is, the impurity "pins" a cluster, (a region the size of the coherence length in which the lattice takes one or the other of its low-temperature configurations) stabilizing a local region in one configuration of the ordered phase. Below T^* this cluster remains fixed in that configuration but grows in size. This latter feature, as the authors emphasized, is certainly a result of the mean-field treatment and it cannot be expected that the decay of the cluster comes to a complete halt. It seems clear however that, experimentally and theoretically, impurities (such as those which cause a local slowing-down of the motion) can slow down the motion of the clusters in their vicinity by orders of magnitude which explains the narrow and, so far, unobserved width of the central peak. We note that the Fe^{3+}-V_O site which we use as a probe, is unlikely to be the cause of the slowing-down since the absence of the oxygen atom will lower the moment of inertia of the octahedron and tend to raise its natural rotation frequency. In this model, one might expect that the measured $P(\phi)$ would be characteristic of the intrinsic material, the impurities serving only to "freeze-in" the fluctuations.

We note that Halperin and Varma[26] have given a theory for the effect of impurities that couple linearly to the order parameter that leads to a central peak whose strength is proportional to the concentration. The relaxation time in their model is fixed, however, and does not go to zero as does the Höck-Thomas calculation, inasmuch as no attempt is made to determine the impurity dynamics self-consistently. More recently, Schmidt and Schwabl[27] sketched a theory in which the impurity couples quadratically to the order parameter which contains the slowing down of the clusters and leads as well to a central peak whose intensity is proportional to the density of impurities. A theory sufficient to explain in detail the probability distribution of local fields remains to be given.

The present study has narrowed down the width of the central peak below the value of 20 MHz or 0.08 μeV, obtained by Töpler *et al.*[3] with a refined neutron back-scattering technique over the same temperature range of $T_c < T < T_c + 12$ K. The latter result agrees with the γ-ray scattering results of Darlington *et al.*[28] whereas the upper limit from light scattering is 300 MHz.[29] Note, however, that the different techniques probe different properties of the crystal. For instance, X- and γ-ray analysis is obtained from highly perturbed surface regions of the crystal. On the other hand, the EPR lines result from only slightly disturbed parts of the crystal. Too strong disturbances cause the lines to shift so much that they cannot contribute to the line intensity. Inelastic neutron diffraction experiments integrate over all defects giving an intensity at the R point.

Recent inelastic neutron experiments showed that the central peak is sample dependent.[30] Most recently Hastings, Shapiro, and Frazer[31] observed a systematic enhancement of the central-peak intensity upon reduction of $SrTiO_3$ with hydrogen. The results provide direct experimental evidence for the involvement of a defect mechanism for the central-peak formation in $SrTiO_3$. However, on approaching T_c, the soft mode ω_∞ is the same in all samples and agrees with the extrapolated low-temperature value obtained from diffuse light scattering of 0.13 THz.[29] The interplay of impurity and intrinsic effects at the structural phase transition is evidently rather subtle. At T_c the wings of the EPR line fall even more steeply than a Gaussian (even steeper than in Fig. 14). Most recently Bruce, Müller, and Berlinger[32] analyzed that shape, i.e., the probability function $P(\phi)$ according to the present findings, in terms of a superposition of a discontinuous Ising variable $\pm\delta_0$ and a Gaussian random variable $Y(t)$; $\phi(t) = \pi_a(t) + Y(t)$. They obtained a value of $\delta_0 = 0.22°$ exposing the local *order-disorder* character of long-lived clusters at T_c. The amount δ_0 found, is in quantitative agreement with the nonvanishing soft mode mentioned above through the empirical relation[33] $\omega_s = 0.69\langle\phi\rangle \approx 0.15$ THz. The non-Gaussian distribution at T_c cannot be obtained from the results in Sec. V, where it is assumed that the effects of the impurities are independent and additive. Within the pinned cluster model one would have to include correlations between clusters and/or nonlinear effects.

ACKNOWLEDGMENT

The work done by one of us (P.H.) at Brandeis University was supported by NSF.

APPENDIX A: DERIVATION OF LINEWIDTH IN THE FAST LIMIT

We wish to derive the expression for the linewidth in the fast regime. A general expression for the spectral function has been attained in Ref. 16. If the rf field is aligned along the y axis the measured spectral function is

$$I(\omega) = \int_0^\infty e^{i(\omega+i\epsilon)t} \langle S^y | V(t) | S^y \rangle \, dt \;, \tag{A1}$$

where

$$\frac{\partial}{\partial t} V_{ij}(t) - iL_i \bar{V}_{ij}(t) + \int_0^t K_{ik}(t-t') \langle \phi_y(t)\phi_y(t') \rangle \times V_{kj}(t')\, dt' = \delta(t)\delta_{ij} \;, \tag{A2}$$

with $t_0 = 0$ in Eq. (17) of that work.

The notation is the same as Ref. 16. For the case under consideration, the separation between the lines due to different transitions $|\mathcal{L}_i - \mathcal{L}_2|$ is of the order of 10^{10} Hz whereas the linewidths are of the order of 10^7 Hz. Barring an accidental degeneracy not observed to occur (for the resonance with which we are concerned, there are no cross-relaxation processes to be considered) K_{ik} may be taken as diagonal; V_{ij} in this case is a diagonal matrix and Eq. (A2) may be readily solved,

$$V_{ii}(\omega) = i / [\omega - \mathcal{L}_i + i\tilde{k}(\omega)] \;, \tag{A3}$$

where

$$\tilde{K}(\omega) = \int_0^\infty e^{i\omega t} K_{ii}(t) \langle \phi_y(t)\phi_y(0) \rangle \, dt \;. \tag{A4}$$

The spectral function is

$$I(\omega) = i |\langle S_y | i \rangle|^2 [\omega - \mathcal{L}_i + i\tilde{K}(\omega)]^{-1} \;. \tag{A5}$$

The assumption that the decay of $\langle\phi_y(t)\phi_y(0)\rangle$ is rapid compared with the linewidth, means that $\tilde{K}(\omega) \simeq \tilde{K}(\mathcal{L}_i)$ over a range of frequencies of the order of the linewidth, and hence the linewidth γ_i is merely

$$\gamma_i = \mathrm{Re}\tilde{K}(\mathcal{L}_i) \;. \tag{A6}$$

If we denote the eigenstates of the ion Hamiltonian by $|\alpha)$, i.e., $\mathcal{H}_I|\alpha) = E_\alpha|\alpha)$, then the state $|i\rangle$ corresponds to the operator $|\alpha)(\beta|$ and

$$L|i\rangle = L_i|i\rangle = \frac{1}{\hbar}[H, |\alpha)(\beta|] = (E_\alpha - E_\beta)/\hbar \, |\alpha)(\beta| \;, \tag{A7}$$

identifying $\mathcal{L}_i$ as $(E_\alpha - E_\beta)/\hbar$.

The matrix $K_{ii}(t)$ is defined as

$$K_{ii}(t)=\Delta_{ij}e^{i\mathcal{L}_j t}\Delta_{ji} \ , \tag{A8}$$

where

$$\Delta_{ij}=T_r O_i[O_y,O_j] \ . \tag{A9}$$

O_i is one of the operators $|\alpha)(\beta|$, and $O_y=D(S_xS_z+S_zS_x)$. Denoting the ground state by $|\alpha_0)$, the first excited state by $|\alpha_1)$ and setting $|1\rangle=|\alpha_0)(\alpha_1|$, $|j\rangle=|\alpha)(\beta|$, we have

$$\begin{aligned}\Delta_{i,j}&=\delta_{\alpha_0\beta}(\alpha_1|O_y|\alpha)-\delta_{\alpha_1\alpha}(\beta|O_y|\alpha_0) \ ,\\ \Delta_{j,i}&=\delta_{\alpha_0\beta}(\alpha|O_y|\alpha_1)-\delta_{\alpha_1\alpha}(\alpha_0|O_y|\beta) \ .\end{aligned} \tag{A10}$$

Equations (A4), (A6), (A8), and (A10) imply

$$\begin{aligned}\gamma_1=&\sum_{\alpha\neq\alpha_0}|(\alpha_0|O_y|\alpha)|^2J_y(E_\alpha-E_{\alpha_0})\\ &+\sum_{\alpha\neq\alpha_1}|(\alpha_1|O_y|\alpha)|^2J_y(E_\alpha-E_{\alpha_1})\\ &+[(\alpha_0|O_y|\alpha_0)-(\alpha_1|O_y|\alpha_1)]^2J_y(0) \ .\end{aligned} \tag{A11}$$

If one now adds the contribution from rotation in the x direction [assuming $\langle\phi_x(t)\phi_y(0)\rangle=0$] one obtains, with a change of notation, Eq. (5) of the text.

APPENDIX B: EFFECT OF NONSECULAR RELAXATION ON THE LINE SHAPE

We wish to show that Eq. (9) describes the relaxation function in the case we are considering. In general, a simple result such as this will not hold if both secular and nonsecular relaxations exist. It holds, in this case, because the linewidth and the characteristic relaxation frequency for the secular fluctuations are several orders of magnitude smaller than both the relaxation frequency of the fluctuations responsible for the nonsecular broadening, and the separation between the excitation energies of the ion.

Here, we will use the terminology of Ref. 16. The contribution to $K_{11}(\omega)$, that yields the nonsecular linewidth is shown in Fig. 15(a). There are no higher-order contributions of significance as these are smaller by factors of the nonsecular linewidth in text (nonsecular relaxation frequency or energy-level separation), which is, in this case, on the order of 10^{-3}. There are, in addition, nonsecular contributions that can appear in intermediate states of diagrams that would otherwise contribute only to the secular self-energy, such as Fig. 15(b). These are also negligible compared to the same diagrams with all intermediate states being $|1\rangle$, with the exception of such diagrams as those of Fig. 15(c).

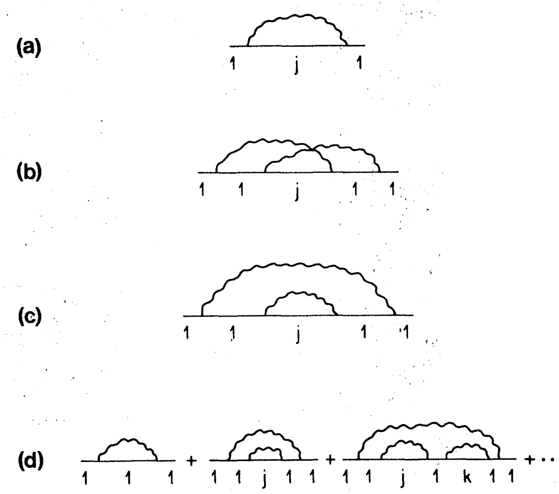

FIG. 15. Contributions to the self-energy of the EPR resonance due to nonsecular terms ($J,K\neq1$).

These are related to the value of the same diagram without the self-energy insertion by $\gamma_{\mathrm{NS}}/(\omega-\omega_0)$, and consequently, are comparable to the original diagram for ω near the resonance frequency. One must include all such insertions in any line of a given diagram. This is accomplished by replacing ω by $\omega+i\gamma_{\mathrm{NS}}$ in the analytic expressions for the secular self-energy. In this way, for instance, all the diagrams of Fig. 15(d) are summed. (We ignore a small frequency shift which is also present.) The result for $K_{11}(\omega)$ is then simply

$$K_{11}(\omega)=\Phi(\omega+i\gamma_{\mathrm{NS}})+i\gamma_{\mathrm{NS}} \ , \tag{B1}$$

where $\Phi(\omega)$ is the sum of all the secular diagrams. Equation (9) is the result.

APPENDIX C: ELEMENTARY DERIVATION OF A FREQUENCY-INTEGRAL FORMULA FOR THE PROBE RELAXATION FUNCTION

Consider an ensemble of classical spins precessing in a field $[H_0+h(t)]\hat{1}_z$ where $h(t)$ is a random field (with zero mean). Let all the spins be initially oriented along the x direction. We seek an expression for $R(t)$, the ratio of the length of the ensemble average magnetization at time t to its $t=0$ value. Our starting point is the general Kubo-Tomita result

$$R(t)=e^{-\psi(t)} \ , \tag{C1}$$

where

$$\psi(t)=\tfrac{1}{2}\sigma_\theta^2(t)=\tfrac{1}{2}\langle\Delta\theta\rangle^2 \tag{C2}$$

is one half the mean-square angular variance at time t. We wish to relate this to the power density spectrum of the random field.

To begin with let us suppose that $h(t)$ merely had two Fourier components, i.e., at a particular spin in the ensemble

$$h(t)=h_1\cos(\omega_1 t+\phi_1)+h_2\cos(\omega_2 t+\phi_2)\quad . \tag{C3}$$

We suppose that a similar formula holds for every spin in the ensemble, assuming that while the frequencies ω_1 and ω_2 have the same two values for all spins, the phases ϕ_1 and ϕ_2 are random. (This means in particular that ϕ_1 is uniformly distributed from 0 to 2π, and is not correlated with h_1, ϕ_2, or h_2.)

Focusing first on a particular spin, we calculate the difference between its actual Larmor precession angle at time t and the mean-precession angle $\bar{\theta}(t)=\gamma H_0 t$. This difference is easily seen to be

$$\begin{aligned}\Delta\theta(t)&=\int_0^t \gamma h(t')\,dt'\\&=\frac{\gamma h_1}{\omega_1}[\sin(\omega_1 t+\phi_1)-\sin\phi_1]\\&\quad+\frac{\gamma h_2}{\omega_2}[\sin(\omega_2 t+\phi_2)-\sin\phi_2]\quad .\end{aligned} \tag{C4}$$

Now it is convenient to rewrite the square-bracketed terms as follows: we have, for example,

$$\sin(\omega_1 t+\phi_1)-\sin\phi_1=2\sin\left(\frac{\omega_1 t}{2}\right)\cos\left(\frac{\omega_1 t}{2}+\phi_1\right)\quad . \tag{C5}$$

From this, and our assumptions about the phases, we see that

$$\langle[\Delta\theta(t)]^2\rangle=4\left\langle\frac{1}{2}\left(\frac{\gamma h_1}{\omega_1}\right)^2\sin^2\frac{\omega_1 t}{2}+\frac{1}{2}\left(\frac{\gamma h_2}{\omega_2}\right)^2\sin^2\frac{\omega_2 t}{2}\right\rangle\quad . \tag{C6}$$

Now it is easy to generalize this model to one in which the local field consists of infinitely many sinusoidally oscillating terms. If the set of frequencies is denoted by $\omega_1, \omega_2, \omega_3\ldots$, we see that

$$\begin{aligned}\psi(t)&=\tfrac{1}{2}\langle[\Delta\theta(t)]^2\rangle\\&=2\gamma^2\sum_i\left\langle\frac{1}{2}h_i^2\frac{\sin^2\frac{1}{2}\omega_i t}{\omega_i^2}\right\rangle\quad .\end{aligned} \tag{C7}$$

Now by definition of the power density spectrum, the contribution to the sum on the right in Eq. (C7) for frequencies in the range ω to $\omega+d\omega$ is

$$\gamma^2 J_h(\omega)\frac{\sin^2\frac{1}{2}(\omega t)}{\omega^2}\,d\omega\quad . \tag{C8}$$

Hence, integrating over all frequencies

$$\begin{aligned}\psi(t)&=\tfrac{1}{2}\langle[\Delta\theta(t)]^2\rangle\\&=2\gamma^2\int_{-\infty}^{\infty}J_h(\omega)\frac{\sin^2\frac{1}{2}(\omega t)}{\omega^2}\,d\omega\quad .\end{aligned} \tag{C9}$$

This may be written

$$\psi(t)=\gamma^2\int_{-\infty}^{\infty}J_h(\omega)\left(\frac{1-\cos\omega t}{\omega^2}\right)d\omega\quad . \tag{C10}$$

This corresponds to the secular term in Eq. (10). [Note our notation here in which the total local-field fluctuation is $\langle h^2\rangle=\int_{-\infty}^{\infty}J_h(\omega)\,d\omega$.] Note that $\gamma=d\theta/dh$ is clearly equivalent to the parameter $B(\theta)$ that describes the sensitivity of the instantaneous Larmor precession rate to changes in the local field.

---

*Present address: Physics Dept., Brookhaven National Laboratory, Upton, N.Y. 11973. Part of this work was done while the author was a visitor at Texas A & M University.

[1]T. Riste, E. J. Samuelsen, K. Otnes, and J. Feder, Solid State Commun. 9, 1455 (1971).

[2]S. M. Shapiro, J. D. Axe, G. Shirane, and T. Riste, Phys. Rev. B 6, 4332 (1972).

[3]J. Töpler, B. Alefeld, and A. Heidemann, J. Phys. C 10, 635 (1977); in this paper proper reference to previous work has been given.

[4]R. A. Cowley, Ferroelectrics 6, 163 (1974); F. Schwabl, in *Proceedings of the NATO Advanced Study Institute on Anharmonic Lattices, Structural Phase Transitions and Melting*, edited by T. Riste (Noordhoff, Leiden, 1974), p. 87; J. Feder, in *Local Properties at Phase Transitions*, edited by K. A. Müller and A. Rigamonti (North-Holland, Amsterdam, 1976), p. 312.

[5]K. A. Müller, IBM Research Report No. RZ 892 (unpublished).

[6]Th. von Waldkirch, K. A. Müller, and W. Berlinger, Phys. Rev. B 5, 4324 (1972).

[7]The measured width is actually that of the local fluctuation $\phi(r)=\sum e^{i\vec{q}\cdot\vec{r}_i}\phi_q$. With reasonable assumptions (see Ref. 14) on the dispersion in the vicinity of the critical wave vector q_c the linewidth of $q=q_c$ will be smaller by another factor of approximately 10, giving an estimate of less than 0.6 MHz for the linewidth of the central peak.

[8]W. Berlinger and K. A. Müller, Rev. Sci. Instrum. 48, 1161 (1977).

[9]Montedel Laben Div., Milano.

[10]K. A. Müller, W. Berlinger, M. Capizzi, and H. Gränicher, Solid State Commun. 8, 549 (1970).

[11]E. S. Kirkpatrick, K. A. Müller, and R. S. Rubins, Phys. Rev. 135, A86 (1964).

[12]G. F. Reiter, W. Berlinger, T. Schneider, and K. A. Müller, in *Proceedings of the 18th Conference on Magnetic Resonance and Related Phenomena,* edited by P. S. Allen, E. R. Andrew, and C. A. Bates (University of Nottingham, England, 1974), Vol. 2, p. 309.

[13]G. W. Smith, J. Appl. Phys. 35, 1217 (1964).

[14]K. A. Müller, W. Berlinger, C. H. West, and P. Heller, Phys. Rev. Lett. 32, 160 (1974); R. Folk and F. Schwabl, Solid State Commun. 15, 937 (1974).

[15]Th. von Waldkirch, K. A. Müller, and W. Berlinger, Phys. Rev. B 7, 1052 (1973).

[16]G. F. Reiter, Phys. Rev. B 9, 3780 (1974).

[17]R. Kubo and K. Tomita, J. Phys. Soc. Jpn. 9, 888 (1954).

[18]T. Schneider and E. Stoll, Phys. Rev. Lett. 31, 1254 (1973); Phys. Rev. B 13, 1216 (1976).

[19]K. A. Müller and W. Berlinger (unpublished).

[20]A. D. Bruce and T. Schneider, Phys. Rev. B 16, 3991 (1977).

[21]K. A. Müller and W. Berlinger, Phys. Rev. Lett. 26, 13 (1971).

[22]A. M. Stoneham, Rev. Mod. Phys. 41, 82 (1969).

[23]J. D. Axe, S. M. Shapiro, G. Shirane, and T. Riste, in *Proceedings of the NATO Advanced Study Institute on Anharmonic Lattices, Structural Phase Transitions and Melting,* edited by T. Riste (Noordhoff, Leiden, 1974), p. 23.

[24]K. A. Müller and W. Berlinger, Z. Phys. B 31, 151 (1978).

[25]K. H. Höck and H. Thomas, Z. Phys. 27, 267 (1977).

[26]B. I. Halperin and C. M. Varma, Phys. Rev. B 14, 4030 (1976).

[27]H. Schmidt and F. Schwabl, Phys. Lett. A 61, 476 (1977).

[28]C. N. W. Darlington, W. J. Fitzgerald, and D. A. O'Connor, Phys. Lett. A 54, 35 (1975).

[29]K. B. Lyons and P. A. Fleury, Solid State Commun. 23, 477 (1977).

[30]R. Currat, K. A. Müller, W. Berlinger, and F. Denoyer, Phys. Rev. B 17, 2937 (1978).

[31]J. B. Hastings, S. M. Shapiro, and B. C. Frazer, Phys. Rev. Lett. 40, 237 (1978).

[32]A. D. Bruce, K. A. Müller, and W. Berlinger, Phys. Rev. Lett. 42, 185 (1979).

[33]E. F. Steigmeier and H. Auderset, Solid State Commun. 12, 565 (1973).